FERMILAB-PUB-07/588-E

Model-independent measurement of the W boson helicity in top quark decays at D0

V.M. Abazov[36], B. Abbott[76], M. Abolins[66], B.S. Acharya[29], M. Adams[52], T. Adams[50], E. Aguilo[6], S.H. Ahn[31], M. Ahsan[60], G.D. Alexeev[36], G. Alkhazov[40], A. Alton[65,a], G. Alverson[64], G.A. Alves[2], M. Anastasoaie[35], L.S. Ancu[35], T. Andeen[54], S. Anderson[46], B. Andrieu[17], M.S. Anzelc[54], Y. Arnoud[14], M. Arov[61], M. Arthaud[18], A. Askew[50], B. Åsman[41], A.C.S. Assis Jesus[3], O. Atramentov[50], C. Autermann[21], C. Avila[8], C. Ay[24], F. Badaud[13], A. Baden[62], L. Bagby[53], B. Baldin[51], D.V. Bandurin[60], S. Banerjee[29], P. Banerjee[29], E. Barberis[64], A.-F. Barfuss[15], P. Bargassa[81], P. Baringer[59], J. Barreto[2], J.F. Bartlett[51], U. Bassler[18], D. Bauer[44], S. Beale[6], A. Bean[59], M. Begalli[3], M. Begel[72], C. Belanger-Champagne[41], L. Bellantoni[51], A. Bellavance[51], J.A. Benitez[66], S.B. Beri[27], G. Bernardi[17], R. Bernhard[23], I. Bertram[43], M. Besançon[18], R. Beuselinck[44], V.A. Bezzubov[39], P.C. Bhat[51], V. Bhatnagar[27], C. Biscarat[20], G. Blazey[53], F. Blekman[44], S. Blessing[50], D. Bloch[19], K. Bloom[68], A. Boehnlein[51], D. Boline[63], T.A. Bolton[60], G. Borissov[43], T. Bose[78], A. Brandt[79], R. Brock[66], G. Brooijmans[71], A. Bross[51], D. Brown[82], N.J. Buchanan[50], D. Buchholz[54], M. Buehler[82], V. Buescher[22], V. Bunichev[38], S. Burdin[43,b], S. Burke[46], T.H. Burnett[83], C.P. Buszello[44], J.M. Butler[63], P. Calfayan[25], S. Calvet[16], J. Cammin[72], W. Carvalho[3], B.C.K. Casey[51], N.M. Cason[56], H. Castilla-Valdez[33], S. Chakrabarti[18], D. Chakraborty[53], K.M. Chan[56], K. Chan[6], A. Chandra[49], F. Charles[19,‡], E. Cheu[46], F. Chevallier[14], D.K. Cho[63], S. Choi[32], B. Choudhary[28], L. Christofek[78], T. Christoudias[44,†], S. Cihangir[51], D. Claes[68], Y. Coadou[6], M. Cooke[81], W.E. Cooper[51], M. Corcoran[81], F. Couderc[18], M.-C. Cousinou[15], S. Crépé-Renaudin[14], D. Cutts[78], M. Ćwiok[30], H. da Motta[2], A. Das[46], G. Davies[44], K. De[79], S.J. de Jong[35], E. De La Cruz-Burelo[65], C. De Oliveira Martins[3], J.D. Degenhardt[65], F. Déliot[18], M. Demarteau[51], R. Demina[72], D. Denisov[51], S.P. Denisov[39], S. Desai[51], H.T. Diehl[51], M. Diesburg[51], A. Dominguez[68], H. Dong[73], L.V. Dudko[38], L. Duflot[16], S.R. Dugad[29], D. Duggan[50], A. Duperrin[15], J. Dyer[66], A. Dyshkant[53], M. Eads[68], D. Edmunds[66], J. Ellison[49], V.D. Elvira[51], Y. Enari[78], S. Eno[62], P. Ermolov[38], H. Evans[55], A. Evdokimov[74], V.N. Evdokimov[39], A.V. Ferapontov[60], T. Ferbel[72], F. Fiedler[24], F. Filthaut[35], W. Fisher[51], H.E. Fisk[51], M. Ford[45], M. Fortner[53], H. Fox[23], S. Fu[51], S. Fuess[51], T. Gadfort[71], C.F. Galea[35], E. Gallas[51], E. Galyaev[56], C. Garcia[72], A. Garcia-Bellido[83], V. Gavrilov[37], P. Gay[13], W. Geist[19], D. Gelé[19], C.E. Gerber[52], Y. Gershtein[50], D. Gillberg[6], G. Ginther[72], N. Gollub[41], B. Gómez[8], A. Goussiou[56], P.D. Grannis[73], H. Greenlee[51], Z.D. Greenwood[61], E.M. Gregores[4], G. Grenier[20], Ph. Gris[13], J.-F. Grivaz[16], A. Grohsjean[25], S. Grünendahl[51], M.W. Grünewald[30], J. Guo[73], F. Guo[73], P. Gutierrez[76], G. Gutierrez[51], A. Haas[71], N.J. Hadley[62], P. Haefner[25], S. Hagopian[50], J. Haley[69], I. Hall[66], R.E. Hall[48], L. Han[7], P. Hansson[41], K. Harder[45], A. Harel[72], R. Harrington[64], J.M. Hauptman[58], R. Hauser[66], J. Hays[44], T. Hebbeker[21], D. Hedin[53], J.G. Hegeman[34], J.M. Heinmiller[52], A.P. Heinson[49], U. Heintz[63], C. Hensel[59], K. Herner[73], G. Hesketh[64], M.D. Hildreth[56], R. Hirosky[82], J.D. Hobbs[73], B. Hoeneisen[12], H. Hoeth[26], M. Hohlfeld[22], S.J. Hong[31], S. Hossain[76], P. Houben[34], Y. Hu[73], Z. Hubacek[10], V. Hynek[9], I. Iashvili[70], R. Illingworth[51], A.S. Ito[51], S. Jabeen[63], M. Jaffré[16], S. Jain[76], K. Jakobs[23], C. Jarvis[62], R. Jesik[44], K. Johns[46], C. Johnson[71], M. Johnson[51], A. Jonckheere[51], P. Jonsson[44], A. Juste[51], E. Kajfasz[15], A.M. Kalinin[36], J.R. Kalk[66], J.M. Kalk[61], S. Kappler[21], D. Karmanov[38], P.A. Kasper[51], I. Katsanos[71], D. Kau[50], R. Kaur[27], V. Kaushik[79], R. Kehoe[80], S. Kermiche[15], N. Khalatyan[51], A. Khanov[77], A. Kharchilava[70], Y.M. Kharzheev[36], D. Khatidze[71], T.J. Kim[31], M.H. Kirby[54], M. Kirsch[21], B. Klima[51], J.M. Kohli[27], J.-P. Konrath[23], V.M. Korablev[39], A.V. Kozelov[39], D. Krop[55], T. Kuhl[24], A. Kumar[70], S. Kunori[62], A. Kupco[11], T. Kurča[20], J. Kvita[9,†], F. Lacroix[13], D. Lam[56], S. Lammers[71], G. Landsberg[78], P. Lebrun[20], W.M. Lee[51], A. Leflat[38], F. Lehner[42], J. Lellouch[17], J. Leveque[46], J. Li[79], Q.Z. Li[51], L. Li[49], S.M. Lietti[5], J.G.R. Lima[53], D. Lincoln[51], J. Linnemann[66], V.V. Lipaev[39], R. Lipton[51], Y. Liu[7,†], Z. Liu[6], A. Lobodenko[40], M. Lokajicek[11], P. Love[43], H.J. Lubatti[83], R. Luna[3], A.L. Lyon[51], A.K.A. Maciel[2], D. Mackin[81], R.J. Madaras[47], P. Mättig[26], C. Magass[21], A. Magerkurth[65], P.K. Mal[56], H.B. Malbouisson[3], S. Malik[68], V.L. Malyshev[36], H.S. Mao[51], Y. Maravin[60], B. Martin[14], R. McCarthy[73], A. Melnitchouk[67], L. Mendoza[8], P.G. Mercadante[5], M. Merkin[38], K.W. Merritt[51], J. Meyer[22,d], A. Meyer[21], T. Millet[20], J. Mitrevski[71], J. Molina[3], R.K. Mommsen[45], N.K. Mondal[29], R.W. Moore[6], T. Moulik[59], G.S. Muanza[20], M. Mulders[51], M. Mulhearn[71], O. Mundal[22], L. Mundim[3], E. Nagy[15], M. Naimuddin[51], M. Narain[78], N.A. Naumann[35], H.A. Neal[65], J.P. Negret[8], P. Neustroev[40], H. Nilsen[23], H. Nogima[3], S.F. Novaes[5], T. Nunnemann[25], V. O'Dell[51], D.C. O'Neil[6], G. Obrant[40], C. Ochando[16], D. Onoprienko[60], N. Oshima[51], J. Osta[56], R. Otec[10], G.J. Otero y Garzón[51], M. Owen[45], P. Padley[81], M. Pangilinan[78], N. Parashar[57], S.-J. Park[72], S.K. Park[31], J. Parsons[71], R. Partridge[78], N. Parua[55], A. Patwa[74], G. Pawloski[81], B. Penning[23], M. Perfilov[38], K. Peters[45], Y. Peters[26], P. Pétroff[16], M. Petteni[44], R. Piegaia[1], J. Piper[66], M.-A. Pleier[22], P.L.M. Podesta-Lerma[33,c], V.M. Podstavkov[51], Y. Pogorelov[56], M.-E. Pol[2], P. Polozov[37], B.G. Pope[66], A.V. Popov[39], C. Potter[6], W.L. Prado da Silva[3], H.B. Prosper[50], S. Protopopescu[74], J. Qian[65], A. Quadt[22,d], B. Quinn[67], A. Rakitine[43], M.S. Rangel[2], K. Ranjan[28], P.N. Ratoff[43],

P. Renkel[80], S. Reucroft[64], P. Rich[45], J. Rieger[55], M. Rijssenbeek[73], I. Ripp-Baudot[19], F. Rizatdinova[77], S. Robinson[44], R.F. Rodrigues[3], M. Rominsky[76], C. Royon[18], P. Rubinov[51], R. Ruchti[56], G. Safronov[37], G. Sajot[14], A. Sánchez-Hernández[33], M.P. Sanders[17], A. Santoro[3], G. Savage[51], L. Sawyer[61], T. Scanlon[44], D. Schaile[25], R.D. Schamberger[73], Y. Scheglov[40], H. Schellman[54], T. Schliephake[26], C. Schwanenberger[45], A. Schwartzman[69], R. Schwienhorst[66], J. Sekaric[50], H. Severini[76], E. Shabalina[52], M. Shamim[60], V. Shary[18], A.A. Shchukin[39], R.K. Shivpuri[28], V. Siccardi[19], V. Simak[10], V. Sirotenko[51], P. Skubic[76], P. Slattery[72], D. Smirnov[56], J. Snow[75], G.R. Snow[68], S. Snyder[74], S. Söldner-Rembold[45], L. Sonnenschein[17], A. Sopczak[43], M. Sosebee[79], K. Soustruznik[9], B. Spurlock[79], J. Stark[14], J. Steele[61], V. Stolin[37], D.A. Stoyanova[39], J. Strandberg[65], S. Strandberg[41], M.A. Strang[70], M. Strauss[76], E. Strauss[73], R. Ströhmer[25], D. Strom[54], L. Stutte[51], S. Sumowidagdo[50], P. Svoisky[56], A. Sznajder[3], M. Talby[15], P. Tamburello[46], A. Tanasijczuk[1], W. Taylor[6], J. Temple[46], B. Tiller[25], F. Tissandier[13], M. Titov[18], V.V. Tokmenin[36], T. Toole[62], I. Torchiani[23], T. Trefzger[24], D. Tsybychev[73], B. Tuchming[18], C. Tully[69], P.M. Tuts[71], R. Unalan[66], S. Uvarov[40], L. Uvarov[40], S. Uzunyan[53], B. Vachon[6], P.J. van den Berg[34], R. Van Kooten[55], W.M. van Leeuwen[34], N. Varelas[52], E.W. Varnes[46], I.A. Vasilyev[39], M. Vaupel[26], P. Verdier[20], L.S. Vertogradov[36], M. Verzocchi[51], F. Villeneuve-Seguier[44], P. Vint[44], P. Vokac[10], E. Von Toerne[60], M. Voutilainen[68,e], R. Wagner[69], H.D. Wahl[50], L. Wang[62], M.H.L.S Wang[51], J. Warchol[56], G. Watts[83], M. Wayne[56], M. Weber[51], G. Weber[24], L. Welty-Rieger[55], A. Wenger[42], N. Wermes[22], M. Wetstein[62], A. White[79], D. Wicke[26], G.W. Wilson[59], S.J. Wimpenny[49], M. Wobisch[61], D.R. Wood[64], T.R. Wyatt[45], Y. Xie[78], S. Yacoob[54], R. Yamada[51], M. Yan[62], T. Yasuda[51], Y.A. Yatsunenko[36], K. Yip[74], H.D. Yoo[78], S.W. Youn[54], J. Yu[79], A. Zatserklyaniy[53], C. Zeitnitz[26], T. Zhao[83], B. Zhou[65], J. Zhu[73], M. Zielinski[72], D. Zieminska[55], A. Zieminski[55,‡], L. Zivkovic[71], V. Zutshi[53], and E.G. Zverev[38]

(The DØ Collaboration)

[1]*Universidad de Buenos Aires, Buenos Aires, Argentina*
[2]*LAFEX, Centro Brasileiro de Pesquisas Físicas, Rio de Janeiro, Brazil*
[3]*Universidade do Estado do Rio de Janeiro, Rio de Janeiro, Brazil*
[4]*Universidade Federal do ABC, Santo André, Brazil*
[5]*Instituto de Física Teórica, Universidade Estadual Paulista, São Paulo, Brazil*
[6]*University of Alberta, Edmonton, Alberta, Canada, Simon Fraser University, Burnaby, British Columbia, Canada, York University, Toronto, Ontario, Canada, and McGill University, Montreal, Quebec, Canada*
[7]*University of Science and Technology of China, Hefei, People's Republic of China*
[8]*Universidad de los Andes, Bogotá, Colombia*
[9]*Center for Particle Physics, Charles University, Prague, Czech Republic*
[10]*Czech Technical University, Prague, Czech Republic*
[11]*Center for Particle Physics, Institute of Physics, Academy of Sciences of the Czech Republic, Prague, Czech Republic*
[12]*Universidad San Francisco de Quito, Quito, Ecuador*
[13]*LPC, Univ Blaise Pascal, CNRS/IN2P3, Clermont, France*
[14]*LPSC, Université Joseph Fourier Grenoble 1, CNRS/IN2P3, Institut National Polytechnique de Grenoble, France*
[15]*CPPM, IN2P3/CNRS, Université de la Méditerranée, Marseille, France*
[16]*LAL, Univ Paris-Sud, IN2P3/CNRS, Orsay, France*
[17]*LPNHE, IN2P3/CNRS, Universités Paris VI and VII, Paris, France*
[18]*DAPNIA/Service de Physique des Particules, CEA, Saclay, France*
[19]*IPHC, Université Louis Pasteur et Université de Haute Alsace, CNRS/IN2P3, Strasbourg, France*
[20]*IPNL, Université Lyon 1, CNRS/IN2P3, Villeurbanne, France and Université de Lyon, Lyon, France*
[21]*III. Physikalisches Institut A, RWTH Aachen, Aachen, Germany*
[22]*Physikalisches Institut, Universität Bonn, Bonn, Germany*
[23]*Physikalisches Institut, Universität Freiburg, Freiburg, Germany*
[24]*Institut für Physik, Universität Mainz, Mainz, Germany*
[25]*Ludwig-Maximilians-Universität München, München, Germany*
[26]*Fachbereich Physik, University of Wuppertal, Wuppertal, Germany*
[27]*Panjab University, Chandigarh, India*
[28]*Delhi University, Delhi, India*
[29]*Tata Institute of Fundamental Research, Mumbai, India*
[30]*University College Dublin, Dublin, Ireland*
[31]*Korea Detector Laboratory, Korea University, Seoul, Korea*
[32]*SungKyunKwan University, Suwon, Korea*
[33]*CINVESTAV, Mexico City, Mexico*
[34]*FOM-Institute NIKHEF and University of Amsterdam/NIKHEF, Amsterdam, The Netherlands*
[35]*Radboud University Nijmegen/NIKHEF, Nijmegen, The Netherlands*
[36]*Joint Institute for Nuclear Research, Dubna, Russia*
[37]*Institute for Theoretical and Experimental Physics, Moscow, Russia*

[38]*Moscow State University, Moscow, Russia*
[39]*Institute for High Energy Physics, Protvino, Russia*
[40]*Petersburg Nuclear Physics Institute, St. Petersburg, Russia*
[41]*Lund University, Lund, Sweden, Royal Institute of Technology and Stockholm University, Stockholm, Sweden, and Uppsala University, Uppsala, Sweden*
[42]*Physik Institut der Universität Zürich, Zürich, Switzerland*
[43]*Lancaster University, Lancaster, United Kingdom*
[44]*Imperial College, London, United Kingdom*
[45]*University of Manchester, Manchester, United Kingdom*
[46]*University of Arizona, Tucson, Arizona 85721, USA*
[47]*Lawrence Berkeley National Laboratory and University of California, Berkeley, California 94720, USA*
[48]*California State University, Fresno, California 93740, USA*
[49]*University of California, Riverside, California 92521, USA*
[50]*Florida State University, Tallahassee, Florida 32306, USA*
[51]*Fermi National Accelerator Laboratory, Batavia, Illinois 60510, USA*
[52]*University of Illinois at Chicago, Chicago, Illinois 60607, USA*
[53]*Northern Illinois University, DeKalb, Illinois 60115, USA*
[54]*Northwestern University, Evanston, Illinois 60208, USA*
[55]*Indiana University, Bloomington, Indiana 47405, USA*
[56]*University of Notre Dame, Notre Dame, Indiana 46556, USA*
[57]*Purdue University Calumet, Hammond, Indiana 46323, USA*
[58]*Iowa State University, Ames, Iowa 50011, USA*
[59]*University of Kansas, Lawrence, Kansas 66045, USA*
[60]*Kansas State University, Manhattan, Kansas 66506, USA*
[61]*Louisiana Tech University, Ruston, Louisiana 71272, USA*
[62]*University of Maryland, College Park, Maryland 20742, USA*
[63]*Boston University, Boston, Massachusetts 02215, USA*
[64]*Northeastern University, Boston, Massachusetts 02115, USA*
[65]*University of Michigan, Ann Arbor, Michigan 48109, USA*
[66]*Michigan State University, East Lansing, Michigan 48824, USA*
[67]*University of Mississippi, University, Mississippi 38677, USA*
[68]*University of Nebraska, Lincoln, Nebraska 68588, USA*
[69]*Princeton University, Princeton, New Jersey 08544, USA*
[70]*State University of New York, Buffalo, New York 14260, USA*
[71]*Columbia University, New York, New York 10027, USA*
[72]*University of Rochester, Rochester, New York 14627, USA*
[73]*State University of New York, Stony Brook, New York 11794, USA*
[74]*Brookhaven National Laboratory, Upton, New York 11973, USA*
[75]*Langston University, Langston, Oklahoma 73050, USA*
[76]*University of Oklahoma, Norman, Oklahoma 73019, USA*
[77]*Oklahoma State University, Stillwater, Oklahoma 74078, USA*
[78]*Brown University, Providence, Rhode Island 02912, USA*
[79]*University of Texas, Arlington, Texas 76019, USA*
[80]*Southern Methodist University, Dallas, Texas 75275, USA*
[81]*Rice University, Houston, Texas 77005, USA*
[82]*University of Virginia, Charlottesville, Virginia 22901, USA and*
[83]*University of Washington, Seattle, Washington 98195, USA*

(Dated: December 11, 2007)

We present the first model-independent measurement of the helicity of W bosons produced in top quark decays, based on a 1 fb^{-1} sample of candidate $t\bar{t}$ events in the dilepton and lepton plus jets channels collected by the D0 detector at the Fermilab Tevatron $p\bar{p}$ Collider. We reconstruct the angle θ^* between the momenta of the down-type fermion and the top quark in the W boson rest frame for each top quark decay. A fit of the resulting $\cos\theta^*$ distribution finds that the fraction of longitudinal W bosons $f_0 = 0.425 \pm 0.166$ (stat.) $\pm\, 0.102$ (syst.) and the fraction of right-handed W bosons $f_+ = 0.119 \pm 0.090$ (stat.) $\pm\, 0.053$ (syst.), which is consistent at the 30% C.L. with the standard model.

PACS numbers: 14.65.Ha, 14.70.Fm, 12.15.Ji, 12.38.Qk, 13.38.Be, 13.88.+e

The top quark is by far the heaviest of the known fermions and is the only one that has a Yukawa coupling to the Higgs boson of order unity in the standard model (SM). In the SM, the top quark decays via the $V - A$ charged-current interaction, almost always to a W boson and a b quark. We search for evidence of new physics in the $t \to Wb$ decay by measuring the helicity of the W boson. A different Lorentz structure of the $t \to Wb$ interaction would alter the fractions of W

bosons produced in each polarization state from the SM values of 0.697 ± 0.012 [1] and 3.6×10^{-4} [2] for the longitudinal fraction f_0 and right-handed fraction f_+, respectively, at the world average top quark mass m_t of 172.5 ± 2.3 GeV [3].

In this Letter, we report a simultaneous measurement of f_0 and f_+ (the negative helicity fraction f_- is then fixed by the requirement that $f_- + f_0 + f_+ = 1$). This is the first model-independent W boson helicity measurement. A measurement of the W boson helicity fractions that differs significantly from the SM values would be an unambiguous indication of new physics [4]-[6]. In addition, the model-independent W boson helicity measurement can be combined with measurements of single top production cross sections to fully specify the tbW vertex [7].

Measurements of the $b \to s\gamma$ decay rate assuming the absence of gluonic penguin contributions have indirectly limited the $V + A$ contribution in top quark decays to less than a few percent [8]. Direct measurements of the longitudinal fraction (f_+ set to zero) found $f_0 = 0.85^{+0.16}_{-0.23}$ [9] and $f_0 = 0.56 \pm 0.31$ [10]. Direct measurements of f_+ (f_0 set to 0.7) have found $f_+ = -0.02 \pm 0.08$ [11] and $f_+ = 0.06 \pm 0.10$ [12]. The analysis presented here improves upon that reported in Ref. [12] by using a larger data set, employing enhanced event selection techniques, making use of hadronic W boson decays, and introducing the model-independent analysis.

The angular distribution of the down-type decay products of the W boson (charged lepton or d, s quark) in the rest frame of the W boson can be described by introducing the decay angle θ^* of the down-type fermion with respect to the top quark direction. The dependence of the distribution of $\cos\theta^*$ on the W boson helicity fractions,

$$\omega(c) \propto 2(1-c^2)f_0 + (1-c)^2 f_- + (1+c)^2 f_+, \qquad (1)$$

where $c = \cos\theta^*$, forms the basis for our measurement. We proceed by selecting a data sample enriched in $t\bar{t}$ events, reconstructing the four vectors of the two top quarks and their decay products, and then calculating $\cos\theta^*$. The down-type fermions in leptonic W boson decays are the charged leptons. For hadronic W boson decays, we choose a W boson daughter jet at random to calculate $\cos\theta^*$. Since this introduces a sign ambiguity into the calculation, we consider only $|\cos\theta^*|$ for hadronic W boson decays. The $|\cos\theta^*|$ variable does not discriminate between left- and right-handed W bosons, but adds information for determining the fraction of longitudinal W bosons. These distributions in $\cos\theta^*$ are compared with templates for different W boson helicity models, accounting for background and reconstruction effects, using a binned maximum likelihood method.

This measurement uses a data sample recorded with the D0 experiment [13] that corresponds to an integrated luminosity of about 1 fb^{-1} of $p\bar{p}$ collisions at $\sqrt{s} = 1.96$ TeV. Events were selected by the trigger system based on the presence of energetic leptons or jets. The data sample consists of $t\bar{t}$ candidate events from the lepton plus jets (ℓ+jets) decay channel $t\bar{t} \to W^+W^-b\bar{b} \to \ell\nu qq'b\bar{b}$ and the dilepton channel $t\bar{t} \to W^+W^-b\bar{b} \to \ell\nu\ell'\nu'b\bar{b}$, where ℓ and ℓ' are electrons or muons. The ℓ+jets final state is characterized by one charged lepton, at least four jets, and large missing transverse energy ($\not\!\!E_T$). The dilepton final state is characterized by two charged leptons, at least two jets, and large $\not\!\!E_T$. In both final states, at least two of the jets are b jets.

The ℓ+jets event selection [14] requires an isolated lepton with transverse momentum $p_T > 20$ GeV, no other lepton with $p_T > 15$ GeV in the event, $\not\!\!E_T > 20$ GeV, and at least four jets. In the dilepton channel, events are required to have two leptons with opposite charge and $p_T > 15$ GeV and two or more jets. Electrons are required to have pseudorapidity [15] $|\eta| < 1.1$ in the ℓ+jets channel and $|\eta| < 1.1$ or $1.5 < |\eta| < 2.5$ in the dilepton channel, and are identified by their energy deposition, isolation, and shower shape in the calorimeter, and information from the tracking system [14]. Muons are identified using information from the muon and tracking systems and must be isolated from jets, significant calorimeter energy, and energetic tracks. They are required to have $|\eta| < 2.0$. Jets are reconstructed using a cone algorithm with cone radius 0.5 [16] and are required to have rapidity $|y| < 2.5$ and $p_T > 20$ GeV. The $\not\!\!E_T$ is calculated from the vector sum of calorimeter cell energies, corrected to account for the response of the calorimeter to jets and electrons and also for the momenta of identified muons.

We simulate $t\bar{t}$ signal events with $m_t = 172.5$ GeV for different values of f_+ with the ALPGEN Monte Carlo (MC) program [17] for the parton-level process (leading order) and PYTHIA [18] for gluon radiation and subsequent hadronization. We generate samples corresponding to each of the three W boson helicity configurations by reweighting the generated $\cos\theta^*$ distributions.

Backgrounds in the ℓ+jets channel arise mainly from W+jets production and multijet production. In the dilepton channel, backgrounds arise from processes such as WW+jets or Z+jets. The MC samples used to model background events with real leptons are also generated using ALPGEN and PYTHIA. Both the signal and background MC samples are passed through a GEANT3 [19] simulation of the detector response and reconstructed with the same algorithms used for data. In the ℓ+jets channel we estimate the number $N_{\rm mj}$ of multijet background events from data, using the technique described in Ref. [14]. We calculate $N_{\rm mj}$ for each bin in the $\cos\theta^*$ distribution from the data sample to obtain the multijet $\cos\theta^*$ templates.

To increase the signal purity, a multivariate likelihood discriminant $\mathcal{D}$ [14] with values in the range 0 to 1 is calculated using input variables which exploit differences in kinematics and jet flavor. The kinematic variables considered are: H_T (scalar sum of the jet p_T values), centrality $\mathcal{C}$ (the ratio of H_T to the sum of the jet energies), $k'_{T\min}$ (the distance in $\eta - \phi$ space between the closest pair of jets multiplied by the E_T of the lowest-E_T jet in the pair and divided by the E_T of the W boson), the sum of all jet and charged lepton energies h, the minimum dijet mass of the jet pairs $m_{jj\min}$, aplanarity $\mathcal{A}$, sphericity $\mathcal{S}$ [20], $\not\!\!E_T$, and the dilepton invariant mass $m_{\ell\ell}$. In the dimuon channel, the χ^2 of a kinematic fit to the $Z \to \mu\mu$

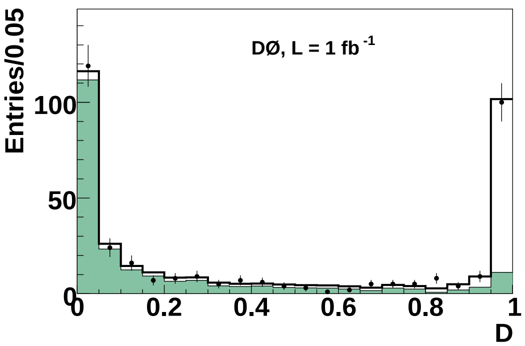

FIG. 1: Distribution of $\mathcal{D}$ for data (points with error bars), background (shaded histogram), and signal plus background (open histogram) in the e+jets channel.

hypothesis χ^2_Z [21] is used instead of $\not\!\!E_T$.

Since jets in background events arise mostly from light quarks or gluons while two of the jets in $t\bar{t}$ events arise from b quarks, we form a neural network discriminant between b and light jets [22] with output value NN_b that tends towards one for b jets and towards zero for light jets.. In the ℓ+jets channels we use the average of the two largest NN_b values to form a continuous variable $\langle NN_b \rangle$ whose value tends to be large for $t\bar{t}$ events and small for backgrounds, while in the dilepton channels the NN_b values for the two leading jets (NN_{b_1}, NN_{b_2}) are taken as separate variables.

The discriminant is built separately for each of the five final states considered, using the method described in Refs. [14, 23]. We consider all possible combinations of the above variables for use in the discriminant, and all possible requirements on the $\mathcal{D}$ value, and choose the variables and $\mathcal{D}$ criterion that give the best expected precision for the W boson helicity. The variables chosen and the requirement placed on $\mathcal{D}$ for each channel are given in Table I. An example of the distributions of signal, background and data events in $\mathcal{D}$ is shown in Fig. 1.

We perform a binned Poisson maximum likelihood fit to compare the observed distribution of events in $\mathcal{D}$ to the sum of the distributions expected from $t\bar{t}$ and background events. In the ℓ+jets channels, $N_{\rm mj}$ is constrained to the expected value within the known uncertainty, while in the dilepton channels the ratio of the various background sources is fixed to the expectation from the cross sections times efficiency of the kinematic selection. The likelihood is then maximized with respect to the numbers of $t\bar{t}$ and background events, which are multiplied by the efficiency for the $\mathcal{D}$ selection to determine the composition of the sample used for measuring the W boson helicity fractions. Table I lists the composition of each sample as well as the number of observed events in the data.

The top quark and W boson four-momenta in the selected ℓ+jets events are reconstructed using a kinematic fit which is subject to the following constraints: two jets must form the invariant mass of the W boson [24], the lepton and the $\not\!\!E_T$ together with the neutrino p_z component must form the invariant mass of the W boson, and the masses of the two reconstructed top quarks must be 172.5 GeV. The four highest-p_T jets in each event are used in the fit, and among the twelve possible jet combinations, the solution with the maximal probability, considering both the χ^2 from the kinematic fit and the NN_b values of the four jets, is chosen. The $\cos\theta^*$ distributions for leptonic and hadronic W boson decays obtained in the ℓ+jets data after the full selection are shown in Fig. 2(a) and (b).

Since the two neutrinos in the dilepton final state are not detected, the system is kinematically underconstrained. However, if m_t is assumed, the kinematics can be solved algebraically with a four-fold ambiguity in addition to the two-fold ambiguity in pairing jets with leptons. For each of the two leading jets, we calculate the value of $\cos\theta^*$ resulting from each solution with each of the two leptons associated with the jet. To explore the phase space consistent with the measured jet and lepton energies, we fluctuate them according to their resolution many times, and repeat the above procedure for each fluctuation. The average of these values is taken as $\cos\theta^*$ for that jet. The $\cos\theta^*$ distribution obtained in dilepton data is shown in Fig. 2(c).

To extract f_0 and f_+, we compute the binned Poisson likelihood $L(f_0, f_+)$ for the data to be consistent with the sum of signal and background templates at any given value for these fractions. The background normalization is constrained to be consistent within uncertainties with the expected value by a Gaussian term in the likelihood. The fit also accounts for the differences in selection efficiency for $t\bar{t}$ events with different W helicity configurations [25].

Systematic uncertainties are evaluated in ensemble tests by varying the parameters that can affect the measurement. Ensembles are formed by drawing events from a model with the parameter under study varied. These are compared to the standard $\cos\theta^*$ templates in a maximum likelihood fit. The average shifts in the resulting f_0 and f_+ values are taken as the systematic uncertainty and are shown in Table II. The total systematic uncertainty is then taken into account in the likelihood by convoluting the likelihood with a Gaussian with a width that corresponds to the total systematic uncertainty. The mass of the top quark is varied by ± 2.3 GeV, and the jet reconstruction efficiency, energy calibration, and b fragmentation parameters by $\pm 1\sigma$ around their nominal values. The $t\bar{t}$ model uncertainty is studied by comparing $t\bar{t}$ events generated by PYTHIA to the standard ALPGEN samples, considering samples with a different model for the underlying event and ones in which only a single primary vertex is reconstructed. Effects of mis-modeling the background distribution in $\cos\theta^*$ are assessed by comparing data to the background model for events with low $\mathcal{D}$ values. The uncertainty due to template statistics is evaluated by fluctuating the templates according to their statistical uncertainties and repeating the fit to the data for each fluctuation. Uncertainties due to jet resolution, jet flavor composition in the background, the modeling of the NN_b variable, and parton distribution functions are all found to be less than 0.01 for both f_0 and f_+.

TABLE I: Summary of the multivariate selection and number of selected events for each of the $t\bar{t}$ final states used in this analysis. The uncertainties are statistical only, except for the background estimates in the ee and $\mu\mu$ channels, in which systematic uncertainties arising from imperfections in the MC model of the data are included.

	e+jets	μ+jets	$e\mu$	ee	$\mu\mu$
Variables used in discriminant $\mathcal{D}$	$\mathcal{C}, \mathcal{S}, \mathcal{A}, H_T$, h, $k'_{T\min}$, $\langle NN_b \rangle$	$\mathcal{C}, \mathcal{S}, H_T$, $k'_{T\min}$, $\langle NN_b \rangle$	$\mathcal{C}, \mathcal{S}, h, m_{jj\min}$, $k'_{T\min}$, NN_{b_1}, NN_{b_2}	$\mathcal{A}, \mathcal{S}$, $k'_{T\min}$, $\not{E}_T$, $m_{\ell\ell}$, NN_{b_1}	$\mathcal{A}, \mathcal{S}$, h, $m_{jj\min}$, χ^2_Z, $m_{\ell\ell}$, NN_{b_1}
Signal purity before $\mathcal{D}$ selection	0.38 ± 0.04	0.44 ± 0.04	0.67 ± 0.11	0.014 ± 0.004	0.024 ± 0.006
Requirement on $\mathcal{D}$	> 0.80	> 0.40	> 0.08	> 0.986	> 0.990
Background after $\mathcal{D}$ selection	21.1 ± 4.5	33.0 ± 5.2	9.9 ± 2.5	2.2 ± 0.9	4.8 ± 3.4
Data events after $\mathcal{D}$ selection	121	167	45	15	15

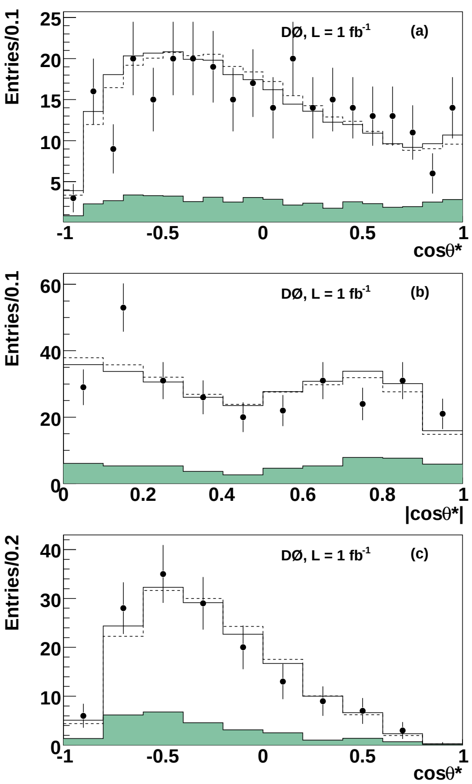

FIG. 2: Comparison of the $\cos\theta^*$ distribution in data (points with error bars) and the global best-fit model (solid open histograms) for (a) leptonic W boson decays in ℓ+jets events, (b) hadronic W boson decays in ℓ+jets events, and (c) dilepton events. The dashed open histograms show the SM expectation, and the shaded histograms represent the background contribution.

TABLE II: Summary of the major systematic uncertainties on f_0 and f_+ in the model-independent fit.

Source	Uncertainty (f_0)	Uncertainty (f_+)
Top mass	0.009	0.018
Jet reconstruction eff.	0.021	0.010
Jet energy calibration	0.012	0.019
b fragmentation	0.016	0.010
$t\bar{t}$ model	0.068	0.032
Background model	0.049	0.016
Template statistics	0.049	0.025
Total	0.102	0.053

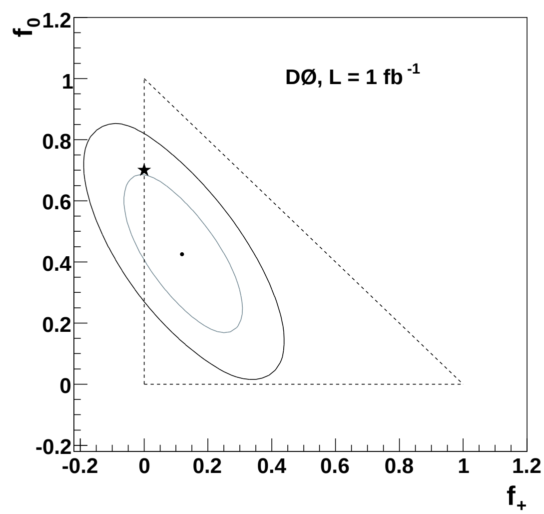

FIG. 3: Result of the model-independent W boson helicity fit. The ellipses are the 68% and 95% C.L. contours, the triangle borders the physically allowed region where f_0 and f_+ sum to one or less, and the star denotes the SM values.

The measured values of f_0 and f_+ are:

$$\begin{aligned} f_0 &= 0.425 \pm 0.166\,\text{(stat.)} \pm 0.102\,\text{(syst.)} \\ f_+ &= 0.119 \pm 0.090\,\text{(stat.)} \pm 0.053\,\text{(syst.)}, \end{aligned} \quad (2)$$

with a correlation coefficient of -0.83. The inclusion of the $|\cos\theta^*|$ measurement from hadronic W boson decays improves the uncertainties on f_0 and f_+ by about 20% relative to those obtained using only the leptonic decays. The 68%, and 95% C.L. contours from the fit, including systematic uncertainties, are shown in Fig. 3. The data indicate fewer longitudinal and more right-handed W bosons than the SM predicts, but the difference is not significant as there is a 30% chance of observing a larger discrepancy given the statistical and systematic uncertainties in the measurement.

If we fix f_+ to the SM value, we find

$$f_0 = 0.619 \pm 0.090\,\text{(stat.)} \pm 0.052\,\text{(syst.)}, \quad (3)$$

and if f_0 is fixed to the SM value we find

$$f_+ = -0.002 \pm 0.047\,\text{(stat.)} \pm 0.047\,\text{(syst.)}. \quad (4)$$

Eqs. 3 and 4 are directly comparable to previous measurements [9]-[12].

In summary, we have measured the helicity fractions of W bosons in $t\bar{t}$ decays in the ℓ+jets and dilepton channels with a model-independent fit and find $f_0 = 0.425 \pm 0.166$ (stat.) $\pm$ 0.102 (syst.) and $f_+ = 0.119 \pm 0.090$ (stat.) $\pm$ 0.053 (syst.). This is the first such measurement reported and is consistent at the 30% level with the SM values of $f_0 = 0.697$ and $f_+ = 3.6 \times 10^{-4}$. We have also measured f_0 and f_+ in a model-dependent fit and find that they are consistent with the SM values.

We thank the staffs at Fermilab and collaborating institutions, and acknowledge support from the DOE and NSF (USA); CEA and CNRS/IN2P3 (France); FASI, Rosatom and RFBR (Russia); CAPES, CNPq, FAPERJ, FAPESP and FUNDUNESP (Brazil); DAE and DST (India); Colciencias (Colombia); CONACyT (Mexico); KRF and KOSEF (Korea); CONICET and UBACyT (Argentina); FOM (The Netherlands); Science and Technology Facilities Council (United Kingdom); MSMT and GACR (Czech Republic); CRC Program, CFI, NSERC and WestGrid Project (Canada); BMBF and DFG (Germany); SFI (Ireland); The Swedish Research Council (Sweden); CAS and CNSF (China); and the Alexander von Humboldt Foundation.

---

[a] Visitor from Augustana College, Sioux Falls, SD, USA.
[b] Visitor from The University of Liverpool, Liverpool, UK.
[c] Visitor from ICN-UNAM, Mexico City, Mexico.
[d] Visitor from II. Physikalisches Institut, Georg-August-University, Göttingen, Germany.
[e] Visitor from Helsinki Institute of Physics, Helsinki, Finland.
[†] Fermilab International Fellow.
[‡] Deceased.

[1] G. L. Kane, G. A. Ladinsky, and C.-P. Yuan, Phys. Rev. D **45**, 124 (1992); R. H. Dalitz and G. R. Goldstein, *ibid.*, 1531; C. A. Nelson *et al.*, Phys. Rev. D **56**, 5928 (1997).
[2] M. Fischer *et al.*, Phys. Rev. D **63**, 031501(R) (2001).
[3] TeVatron Electroweak Working Group, arXiv:hep-ex/0603039 (2006).
[4] J. Cao *et al.*, Phys. Rev. D **68**, 054019 (2003).
[5] Y.M. Nie *et al.*, Phys. Rev. D **71**, 074018 (2005).
[6] X. Wang, Q. Zhang, and Q. Qiao, Phys. Rev. D **71**, 014035 (2005).
[7] C.-R. Chen, F. Larios, and C.-P. Yuan, Phys. Lett. B **631**, 126 (2005); D0 Collaboration, V.M. Abazov *et al.* Phys. Rev. Lett. **98**, 181802 (2007).
[8] K. Fujikawa and A. Yamada, Phys. Rev. D **49**, 5890 (1994); P. Cho and M. Misiak, Phys. Rev. D **49**, 5894 (1994); C. Jessop, SLAC-PUB-9610 (2002).
[9] CDF Collaboration, A. Abulencia *et al.*, Phys. Rev. D **75**, 052001 (2007).
[10] D0 Collaboration, V. M. Abazov *et al.*, Phys. Lett. B **617**, 1 (2005).
[11] CDF Collaboration, A. Abulencia *et al.*, Phys. Rev. Lett. **98**, 072001 (2007).
[12] D0 Collaboration, V. M. Abazov *et al.*, Phys. Rev. D **75**, 031102(R) (2007).
[13] D0 Collaboration, V. M. Abazov *et al.*, Nucl. Instrum. Methods A **565**, 463 (2006).
[14] D0 Collaboration, V. M. Abazov *et al.*, Phys. Lett. B **626**, 45 (2005).
[15] Rapidity y and pseudorapidity η are defined as functions of the polar angle θ with respect to the proton beam and the parameter β as $y(\theta, \beta) \equiv \frac{1}{2} \ln[(1 + \beta \cos\theta)/(1 - \beta\cos\theta)]$ and $\eta(\theta) \equiv y(\theta, 1)$, where β is the ratio of a particle's momentum to its energy.
[16] G.C. Blazey *et al.*, arXiv:hep-ex/0005012 (2000).
[17] M. L. Mangano *et al.*, JHEP **07**, 001 (2003).
[18] T. Sjöstrand *et al.*, Comp. Phys. Commun. **135**, 238 (2001).
[19] S. Agostinelli *et al.*, Nucl. Instrum. Methods A **506**, 250 (2003).
[20] V. Barger *et al.*, Phys. Rev. D **48**, 3953 (1993).
[21] D0 Collaboration, V.M. Abazov *et al.*, Phys. Lett. B **655**, 7 (2007).
[22] T. Scanlon, Ph.D. thesis, University of London; FERMILAB-THESIS-2006-43 (2006).
[23] D0 Collaboration, B. Abbott *et al.*, Phys. Rev. D **58**, 052001 (1998).
[24] Review of Particle Physics, W. M. Yao *et al.*, J. Phys. G **33**, 1 (2006).
[25] D. Glenzinski and B. Kilminster, private communication.